Research Square

Preprints are preliminary reports that have not undergone peer review.
They should not be considered conclusive, used to inform clinical practice,
or referenced by the media as validated information.

OsMYBdt1 Enhances Drought Tolerance in Rice via Antioxidant Defense and ABA Signaling

Guangzhao li
Hunan Agricultural University
Tuo Zhong
Hunan Agricultural University
Yuancheng Sun
Hunan Agricultural University
Chenggang li
China National Hybrid Rice R&D Central Hunan Hybrid Rice Reserch Center
Fenglin Huang
China National Hybrid Rice R&D Central Hunan Hybrid Rice Reserch Center
Shipeng Huang
Hunan Agricultural University
Chuanxin Chen
Hunan Agricultural University
Huqiang He
Hunan Agricultural University
Su Jiang
Hunan Agricultural University
Xin Tian
Hunan Agricultural University
Yue Wang
Hunan Agricultural University
Yajun Hu
Hunan Agricultural University
Guanghui Chen
Hunan Agricultural University
Dan Wang
jessicawangdan@163.com

Hunan Agricultural University

Research Article

Keywords: MYB transcription factor, OsMYBdt1, abscisic acid, drought tolerance, rice

Posted Date: June 17th, 2026

DOI: https://doi.org/10.21203/rs.3.rs-10042328/v1

License: This work is licensed under a Creative Commons Attribution 4.0 International License.
Read Full License

Additional Declarations: No competing interests reported.

Abstract

Rice production is severely constrained by drought stress, which is increasingly exacerbated by climate change. Here, we functionally characterized OsMYBdt1, a previously unstudied MYB transcription factor in rice. CRISPR/Cas9-mediated osmybdt1 knockout mutants exhibited severe drought hypersensitivity, whereas OsMYBdt1-overexpressing (OX) lines demonstrated robustly enhanced tolerance at both vegetative and reproductive stages. Mechanistically, OsMYBdt1 acts as a pivotal regulatory node integrating reactive oxygen species (ROS) homeostasis and abscisic acid (ABA) signaling. Under drought, OsMYBdt1 reinforces the antioxidant network by boosting superoxide dismutase (SOD) and peroxidase (POD) activities, thereby accelerating ROS scavenging. Concurrently, it modulates ABA-dependent stomatal closure to restrict transpirational water loss. The drought-susceptible phenotype of osmybdt1 was fully rescued by exogenous ABA. At the molecular level, molecular docking combined with dual-luciferase transactivation assays elucidated that OsMYBdt1 binds to and transcriptionally activates the promoter of OsRab16A, a Group-2 Late Embryogenesis Abundant gene. Furthermore, haplotype analysis uncovered two major natural variants of OsMYBdt1 exhibiting distinct geographic and ecotypic distribution patterns between indica and japonica subspecies, underscoring its evolutionary divergence under environmental selection. Collectively, our study characterizes OsMYBdt1 as a central regulatory node and provides valuable genetic resources for breeding drought-resilient rice cultivars.

Introduction

Rice (*Oryza sativa* L.) serves as a primary staple crop for more than half of the global population, thereby playing an indispensable role in maintaining global food security. However, rice cultivation is highly water-intensive, rendering it exceptionally susceptible to climate variability and recurrent drought events, both of which are being progressively exacerbated by global climate change (Li et al. 2009; Geng et al. 2015). Severe drought stress substantially suppresses rice grain yields, posing a direct threat to the agricultural economy and food supply chains. To address these challenges, leveraging the inherent morpho-physiological and molecular adaptations of rice via molecular breeding and genetic engineering has emerged as a promising strategy to develop drought-resilient varieties (Sandhu et al. 2019). Consequently, dissecting the intricate molecular mechanisms underlying drought tolerance and accelerating the breeding of climate-resilient cultivars are urgent priorities for sustainable agriculture.

To cope with water deficits, plants have evolved sophisticated, multilayered defense mechanisms orchestrated by interconnected physiological and molecular pathways. Central to these adaptive responses are two highly coordinated systems: reactive oxygen species (ROS) homeostasis and abscisic acid (ABA) signaling networks. Under drought conditions, excessive accumulation of ROS—primarily superoxide radicals ($O_2\bullet^-$) and hydrogen peroxide (H_2O_2)—induces severe oxidative damage to cellular lipids, proteins, and nucleic acids, ultimately compromising cellular integrity (Miller et al. 2010). To counteract this oxidative stress, plants activate an intricate antioxidant defense network comprising scavenging enzymes, such as superoxide dismutase (SOD), peroxidase (POD), and catalase (CAT), to restore cellular redox balance (Nam et al., 2002; Fujita et al., 2005; Cutler et al., 2010; Miller et al., 2010).

overexpression of *FtMYB22* in Arabidopsis disrupts the ROS balance by elevating H_2O_2 and O_2^- levels while suppressing the activities of SOD, POD, and CAT (Zhao et al., 2022). Similarly, in rice, *OsDjC46* and *ZFP36* enhance drought tolerance by regulating SOD and CAT activities through ABA-mediated pathways (Huang et al., 2022).

Concurrently, the phytohormone ABA acts as a core signaling hub that coordinates plant physiological responses to environmental stresses, particularly desiccation (Yoshida et al. 2014). Abiotic stress triggers a rapid accumulation of endogenous ABA, which is perceived by PYR/PYL/RCAR intracellular receptors, ultimately leading to the activation of SnRK2 kinases and downstream transcription factors (TFs) such as AREB/ABFs, DREBs, and MYBs. These TFs, in turn, orchestrate the transcriptomic reprogramming of stress-responsive genes (Wang et al., 2008; Fujii et al., 2009; Umezawa et al., 2009; Yoshida et al., 2014; Lv et al., 2017; Li et al., 2024). Importantly, extensive crosstalk occurs between ROS homeostasis and the ABA signaling cascade. Elevated ROS levels can influence ABA biosynthesis and sensitivity, whereas multiple ABA-responsive downstream genes directly encode ROS-scavenging enzymes (Shinozaki et al., 2007; Yoshida et al., 2014; Gao et al., 2024).

The MYB superfamily represents one of the largest and most functionally diverse TF families in plants, serving as a critical regulatory node in drought adaptation. Several MYB members have been characterized for their roles in drought resistance (Fujita et al., 2005; Yamaguchi et al., 2005; Yang et al., 2012; Yoshida et al., 2014; Baldoni et al., 2015). In Arabidopsis, overexpressing *MYB12* and *MYB75* markedly promotes flavonoid accumulation with potent antioxidant activities (Nakabayashi et al. 2014). In rice, *OsMYB2* enhances osmotic stress tolerance by altering ABA sensitivity (Yang et al. 2012), OsMYB48-1 positively regulates drought responses by upregulating ABA biosynthesis genes (Xiong et al. 2014), and *OsMYB6* participates in the activation of antioxidant defenses (Zhao et al., 2022). Despite the known importance of MYB factors, the specific genetic elements capable of simultaneously balancing ROS detoxification and ABA-mediated stomatal dynamics without severe yield penalties remain poorly understood. (Baldoni et al., 2015; Chen et al., 2021; Peng et al., 2025) Furthermore, the natural variation of such master regulators across diverse rice ecotypes has not been fully explored.

In this study, we functionally characterized *OsMYBdt1* (LOC_Os01g47370), a rice MYB transcription factor previously identified through a GWAS for drought-related traits (Wang et al. 2021), but whose precise molecular mechanism was elusive. Employing CRISPR/Cas9-mediated knockout mutants and stable overexpression lines, we demonstrate that *OsMYBdt1* serves as a crucial positive regulator that robustly enhances drought tolerance. We show that *OsMYBdt1* achieves this via a dual-regulatory mechanism: concurrently bolstering antioxidant enzymatic activities to scavenge ROS and modulating ABA-dependent stomatal closure. Furthermore, we reveal that *OsMYBdt1* directly regulates the transcription of the ABA-responsive gene *OsRab16A*. Collectively, our findings establish OsMYBdt1 as a novel molecular bridge integrating ROS scavenging and ABA signaling, providing both fresh mechanistic insights and a promising genetic target for breeding drought-resilient rice cultivars.

Results

Bioinformatics Characterization and Identification of *OsMYBdt1*

LOC_Os01g47370 was previously identified via a genome-wide association study and designated as *OsMYBdt1* (Wang et al., 2021). Bioinformatics and sequence analyses confirmed that OsMYBdt1 encodes a member of the MYB transcription factor family. The gene contains a 276-bp coding sequence disrupted by a single intron (Fig. 1A). Positive transgenic T_1 rice lines overexpressing *OsMYBdt1* were generated, and two independent lines exhibiting robust overexpression, designated *OsMYBdt1*-OX3 and *OsMYBdt1*-OX6, were selected for functional characterization (Fig. 1B).

Homology modeling using SWISS-MODEL predicted that OsMYBdt1 possesses a conserved, typical MYB DNA-binding domain and a non-conserved regulatory region potentially mediating protein–protein interactions (Fig. 1C). Phylogenetic analysis revealed that OsMYBdt1 clustered closely with OsMYB6, OsMYBS1, and OsMYBS2, suggesting a conserved functional evolution among these related members (Fig. 1D).

Spatiotemporal Expression Profiling and Subcellular Localization of *OsMYBdt1*

Spatial expression analysis via qRT-PCR revealed that *OsMYBdt1* was ubiquitously expressed, with the highest transcript abundance detected in seedling leaves, followed by mature seeds and roots (Fig.2A). *OsMYBdt1* transcripts were significantly induced by 20% PEG6000 (Fig. 2B), 4 μM ABA (Fig. 2C), low temperature (Fig. S1B), high temperature (Fig. 2D), and salinity (Fig. S1A). Notably, *OsMYBdt1* expression peaked rapidly within 1 h post ABA and heat treatments, whereas it exhibited a progressive increase under PEG6000 and cold stress, reaching maximum levels at 36 h and 48 h, respectively. These distinct induction kinetics suggest that *OsMYBdt1* participates in diverse abiotic stress responses through multiple, potentially independent signaling pathways.

Subcellular localization analysis was performed by transiently expressing an OsMYBdt1-GFP fusion construct in rice protoplasts. Confocal microscopy showed that the free GFP control signal was distributed in both the cytoplasm and the nucleus, while the OsMYBdt1-GFP fluorescence signal was detected prominently in the nucleus and also in the cytoplasm, indicating that OsMYBdt1 is a nucleocytoplasmic localized protein (Fig. 2E).

OsMYBdt1 Confers Enhanced Drought Tolerance in Rice

Seedlings at the vegetative stage were subjected to a 14-day osmotic stress treatment using 20% PEG6000, followed by a 7-day recovery period. The survival rates varied markedly among genotypes: the overexpression lines *OsMYBdt1*-OX3 and *OsMYBdt1*-OX6 maintained survival rates exceeding 80%, whereas the knockout mutants *osmybdt1*CR-17 and *osmybdt1*CR-20 exhibited significantly reduced survival rates below 45%, compared to 52.7% observed in the Nipponbare (NPB) wild-type control (Fig. 3A–C). Under basal conditions, no significant morphological differences were detected among genotypes (Figs. S1C, D). However, under PEG-induced stress, the fresh weight of OX lines was significantly higher than that of NPB, while the mutants exhibited a severe reduction in biomass (Figs. S1E, F). Consistently, under natural field drought conditions at the reproductive stage, the OX lines maintained survival rates above 70%, while both NPB and the mutant lines dropped below 25% (Fig. 3B–

D).
We monitored the transcript levels of several stress-responsive marker genes (*OsDERF1, OsLEA3, OsNAC5*, and *OsMYB6*) under both basal and stressed conditions (Fig. 2F–I). Under drought stress, the transcription of the negative regulator *OsDERF1* was significantly repressed in the OX lines compared with NPB and CR mutants (Fig. 2F). Interestingly, the expression levels of *OsLEA3, OsNAC5*, and *OsMYB6* did not show statistically significant differences between the wild-type and transgenic lines under drought conditions (Fig. 2G–I).
Scanning electron microscopy revealed that under drought conditions, the OX lines displayed a significantly higher percentage of fully closed stomata compared to NPB, whereas the knockout lines exhibited a higher proportion of open or partially closed stomata (Fig. 3E, F). These results indicate that *OsMYBdt1* enhances drought tolerance, at least in part, by promoting ABA-dependent stomatal closure to minimize transpirational water loss.

OsMYBdt1 Modulates ABA Signaling Pathways Under Stress

Under well-watered control conditions without ABA, no significant differences in root or shoot length were observed among genotypes. Upon treatment with exogenous ABA (3–5 μM), which uniformly restricted seedling growth, the *OsMYBdt1*-OX lines exhibited significantly longer shoots than the *osmybdt1* mutants and the NPB control after 7 days (Fig. 4A, B). This phenotype likely reflects a reduced apparent sensitivity to the exogenous ABA treatment in the OX lines, which already possessed elevated endogenous ABA levels that pre-adapted them to stress (Fig. 4C). Quantification of endogenous ABA via ELISA confirmed that under drought conditions, the OX lines accumulated significantly higher amounts of ABA than both NPB and the knockout mutants (Fig. 4C).
Remarkably, when the knockout mutant seedlings were pretreated with exogenous ABA prior to 20% PEG6000-induced osmotic stress, their survival rate was fully rescued to approximately 90%, comparable to that of the OX lines (Fig. 4D, E). Collectively, these findings confirm that *OsMYBdt1* functions as a positive regulator required for ABA-mediated drought tolerance, and that the drought-susceptible phenotype of the loss-of-function mutants can be effectively complemented by exogenous ABA.

OsMYBdt1 Enhances ROS Scavenging Activity by Activating Antioxidant Enzymes

Direct water-withholding assays showed that the OX lines consistently achieved higher survival rates than the NPB control and *osmybdt1*CR mutants (Fig. 5A–D). Histochemical staining using trypan blue and DAB revealed extensive cell death and massive ROS accumulation in the mutant lines, moderate accumulation in NPB, and minimal cellular damage in the OX lines (Fig. 5E, F).
Biochemical analysis demonstrated that drought stress significantly boosted peroxidase (POD) and superoxide dismutase (SOD) activities across all genotypes. However, the induction was most pronounced in the OX lines: SOD activity reached 571.5±77.0 U/g FW, significantly higher than that in NPB (280.8±77.1 U/g FW) and the knockout lines (253.3±42.1 U/g FW) (Fig. 5I). POD activity in the OX lines rose to 8320±670 U/g FW (a 5.8-fold induction), significantly outperforming NPB (5680±1090 U/g FW) and the knockout lines (4980±1200 U/g FW) (Fig. 5H). Concurrently, free proline content accumulated to 157.8±8.8 μmol/g FW (a 5.3-fold increase) in the OX lines, representing a significant increase over NPB (121.6±5.8 μmol/g FW) and the CR lines (104.8±8.0 μmol/g FW) (Fig. 5J). In contrast,

malondialdehyde (MDA) content remained relatively constant in the OX lines, whereas the *osmybdt1*CR-17 mutant displayed a significant increase compared to NPB and OX lines (Fig. 5G). These results clearly demonstrate that OsMYBdt1 mitigates drought-induced oxidative damage by reinforcing the endogenous antioxidant enzymatic system and accelerating ROS scavenging.

OsMYBdt1 Directly Regulates the Transcription of *OsRab16A*

To identify the downstream target genes regulated by *OsMYBdt1*, the promoter regions of several stress-related genes were interrogated using the PlantCARE database. Various cis-acting elements associated with MYB binding were identified, including ABREs, MBS, and AREs (Fig. 6A). qRT-PCR analysis showed that the expression levels of *OsNAC6* and *OsRab16A* were markedly upregulated in an *OsMYBdt1*-dependent manner under PEG treatment, marking them as potential targets (Fig. 6B).

Molecular docking simulations using HDOCK predicted that OsMYBdt1 may interact with the *OsRab16A* promoter region, with key residues such as THR-31, GLY-36, and ASP-42 potentially contributing to the interaction interface, and a predicted binding energy of −12.4 kcal/mol (Fig. 6C). To functionally validate this regulation, a dual-luciferase (Dual-LUC) reporter assay was performed (Fig. 6D). Co-expression of the OsMYBdt1 effector with the *proOsRab16A*: LUC reporter led to an approximately 2.0-fold increase in the LUC/REN ratio compared with the empty vector control (Fig. 6F). No activation was observed when OsMYBdt1 was co-expressed with a promoterless LUC vector, confirming that transcriptional activation is strictly dependent on the *OsRab16A* promoter sequence. In vivo luminescence imaging of infiltrated tobacco leaves further showed substantially enhanced firefly luciferase signal only in the OsMYBdt1 + *proOsRab16A*combination (Fig. 6E). Together, these data provide evidence that OsMYBdt1 acts as a direct transcriptional activator of *OsRab16A*.

Influence of *OsMYBdt1* on Agronomic Traits and Haplotype Distribution

We evaluated key agronomic traits across genotypes. No significant differences were observed in plant height or panicle length (Figs. S2A, B). However, the *OsMYBdt1*-OX lines produced a significantly higher number of effective panicles per plant than NPB and the *osmybdt1*CR lines (Fig. S2C). For grain traits, the OX lines displayed an average grain length of 8.5±0.1 mm, which was significantly longer than that of NPB (7.3±0.2 mm; Fig. S2F). Grain width did not differ significantly among the transgenic lines, but both OX and CR lines showed reduced grain width compared to NPB (3.7±0.1 mm; Fig. S2E). The seed-setting rate of the *osmybdt1*CR lines (83.2±6.4%) was unexpectedly higher than that of NPB (71.7±2.7%), while the OX lines (72.2±3.1%) were not significantly different from NPB (Fig. S2D).

Haplotype analysis using the Rice SNP-Seek Database revealed that *OsMYBdt1* exists predominantly as two major haplotypes (Hap1 and Hap2) distinguished by seven non-synonymous amino acid substitutions (Fig. S3A). Hap1 is predominantly restricted to *indica* rice (94.14%) and is widely distributed across tropical and subtropical regions, whereas Hap2 is highly enriched in *japonica* rice (80.93%) and distributed across higher-latitude temperate zones (Fig. S3A, B).

Discussion

OsMYBdt1 is a Conserved Member of the Rice MYB Regulators

The MYB transcription factor family represents one of the largest and most functionally diverse regulatory networks in plants, with at least 183 members identified in rice (*Oryza sativa* L.) that modulate various developmental and stress-adaptive processes (Katiyar et al. 2012; Peng et al. 2025). Although several members, such as OsMYB6, OsMYB48-1, and OsMYB60, have been functionally linked to osmotic stress responses, the precise biological roles of the vast majority of crop MYB factors remain uncharacterized (Liu et al. 2015).

In the present study, we demonstrated that *OsMYBdt1* acts as a robust positive regulator of drought tolerance in rice. Phylogenetic analysis indicated that OsMYBdt1 clusters closely with established stress-responsive MYB proteins, including OsMYB6, OsMYBS1, and OsMYBS2 (Fig. 1D), implying that this specific clade shares a evolutionarily conserved functional paradigm in coordinating survival strategies under adverse environmental conditions.

Dual-Regulatory Node: Synchronized ROS Scavenging and ABA Signaling

A key challenge in crop stress biology is understanding how single regulatory master-switches integrate separate physiological defense systems to mitigate environmental damage without imposing critical growth penalties. Our physiological and biochemical assays demonstrated that the hyper-tolerance of *OsMYBdt1*-OX lines is closely associated with an enhanced cellular antioxidant defense system and highly responsive abscisic acid (ABA) signaling mechanisms. Under water-deficit conditions, *OsMYBdt1* overexpression markedly boosted superoxide dismutase (SOD) and peroxidase (POD) enzymatic activities, promoted free proline accumulation, and limited malondialdehyde (MDA) deposition (Fig. 5G–J). This enzymatic upregulation directly correlated with the restricted accumulation of reactive oxygen species (ROS) (H_2O_2 and $O^{2}\bullet-$) and minimal cell death, as manifested by histochemical staining (Fig. 5E, F). These findings conform to the classical paradigm where specific MYB TFs orchestrate secondary metabolism or enzymatic networks to clear cytotoxic free radicals (Nakabayashi et al. 2014; Wu et al. 2017; Upadhyaya et al. 2021; Zhao et al. 2022).

Concurrently, our genetic evidence strongly places *OsMYBdt1* within the ABA-mediated signaling pathway. The transcript abundance of *OsMYBdt1* responded rapidly to exogenous ABA, whereas its knockout mutants exhibited severe hypersensitivity to ABA-mediated growth restriction during early seedling development (Fig. 4A–D). Crucially, the finding that exogenous ABA supplementation could effectively rescue the drought-sensitive phenotype of osmybdt1 mutant lines (Fig. 4D, E) confirms that *OsMYBdt1* operates, at least in part, via an ABA-dependent cascade. This phenotypic rescue establishes a functional alignment between *OsMYBdt1 a*nd other critical ABA-associated MYB factors, such as *OsMYB48-1* and *MYB96* (Seo et al. 2011; Xiong et al. 2014).

Transcriptional Activation of OsRab16A Bridges Desiccation Tolerance and Enzymatic Protection

At the molecular level, we observed a substantial *OsMYBdt1*-dependent transactivation of *OsRab16A*, a well-characterized Group-2 Late Embryogenesis Abundant (LEA) gene containing multiple stress-responsive cis-acting elements within its promoter region (Mundy and Chua 1988; Ono et al. 1996; Yang

et al. 2012). While previous studies noted that *OsRab16A* expressions can be driven by *OsMYB2* or *OsMYB48-1* (Beittenmiller et al. 1996; Xiong et al. 2014), our structural and biochemical data expand this regulatory hierarchy.

To explore the structural affinity between the OsMYBdt1 transcription factor and the promoter region of *OsRab16A*, molecular docking simulations were conducted utilizing HDOCK software. The simulated structure indicated that multiple crucial amino acid residues, including THR-31, GLY-36, and ASP-42, directly participate in stabilizing the interaction interface (Fig. 6C). Inter-residue distances ranging from 2.5 to 3.3 Å strongly supported the formation of robust hydrogen bonds and hydrophobic interactions, ensuring tight binding. Furthermore, the PRODIGY algorithm predicted a highly favorable binding energy of −12.4 kcal/mol, corroborating a stable interaction complex.

The subsequent in vivo Dual-Luciferase reporter assay demonstrated an approximate 2.0-fold transactivation of proOsRab16A strictly in the presence of the OsMYBdt1 effector (Fig. 6E, F), providing biochemical evidence that OsMYBdt1 acts as a direct upstream transcriptional activator of OsRab16A. Our current molecular docking and in planta transactivation data strongly support OsMYBdt1 as an upstream transcriptional activator of this protective locus, laying the groundwork for future structural validations. Importantly, the direct activation of *OsRab16A* provides a missing logical bridge explaining the concurrent enhancement of antioxidant activities observed in *OsMYBdt1-OX* plants. LEA proteins, including OsRab16A, typically function as macromolecular stabilizers or molecular chaperones that prevent the desiccation-induced denaturation of cellular enzymes. Therefore, we propose that the OsMYBdt1-mediated transcriptional activation of *OsRab16A* not only aids in direct osmotic adjustment but also protects the structural integrity of vital ROS-scavenging enzymes like SOD and POD, allowing them to remain catalytically active under severe water-deficit conditions.

Agronomic Impacts and Haplotype Distribution in Breeding Programs

From an agronomic perspective, a major hurdle in translating stress-tolerance genes into elite crop cultivars is the inherent trade-off between survival mechanisms and grain yield component traits. Interestingly, our phenotypic evaluation revealed that *OsMYBdt1* overexpression significantly enhanced beneficial agronomic characteristics, including effective panicle numbers and grain length, compared to the Nipponbare wild-type (Fig. S2).

Although a minor reduction in grain width and a slight reduction in the seed-setting rate were observed in the OX lines relative to the *osmybdt1* knockouts, the overall increase in panicle number and grain elongation compensates for these parameters, positioning *OsMYBdt1* as a promising target for engineering high-yielding, drought-tolerant varieties without severe yield penalties.

This potential is further supported by our global haplotype assessment using the 3K Genomes dataset. The distinct geographic separation between Hap1 (predominantly conserved in tropical indica varieties across Southeast Asia) and Hap2 (enriched in temperate japonica cultivars in higher latitudes) suggests

that polymorphism variations within the *OsMYBdt1* locus may have undergone rigorous environmental selection during subspecies differentiation.

Further integration of these specific single-nucleotide polymorphisms (SNPs) into marker-assisted selection or gene-editing workflows will facilitate the customized tailoring of climate-resilient rice lines optimized for distinct macroclimatic regions.

In conclusion, *OsMYBdt1* functions as an integrative regulatory hub that couples enhanced antioxidant defense system with ABA-mediated stomatal and transcriptomic signaling to confer comprehensive drought tolerance in rice (Fig. 7F). Its dual capacity to alleviate oxidative injury while promoting the expression of protective down-stream genes highlights the sophisticated, multi-layered defense strategies orchestrated by this transcription factor. Consequently, *OsMYBdt1* stands as an invaluable candidate allele for molecular breeding initiatives aimed at securing cereal production in the face of escalating global drought threats.

Materials and Methods

Plant Growth and Stress Treatment

The rice materials used in this study were of the Nipponbare (NPB) genetic background. Overexpression lines of *OsMYBdt1*, *OsMYBdt1*OX (OX-3, OX-6), and knockout lines of *OsMYBdt1*, *osmybdt1*CR (CR-17, CR-20), were developed in the NPB background. Following germination, the seeds were transplanted into a 96-well PCR-free plate for cultivation. Throughout the cultivation period, rice nutrient solution following Yoshida's recipe was maintained under controlled conditions (12 h light, 12 h dark, 28℃, 70% relative humidity) to ensure optimal growth. Seeds at the mature stage were collected from plants grown in a natural environment and stored at -80℃ for analysis of OsMYBdt1 expression in various tissues including buds, roots, stems, leaves of seedlings, and roots, stems, leaves, inflorescences, and leaf sheaths. For stress-induced expression analysis, 3-week-old seedlings were subjected to 5 different stresses: cold stress (4℃), 100 μmol/L ABA, 150 mmol/L NaCl, high temperature (45℃), and expression patterns after simulated drought stress with 20% PEG-6000. RNA extraction and RT-qPCR analysis were conducted at 0, 0.5, 1, 3, 6, 9, 12, 24, 36 and 48 h after treatment. Three biological replicates were used for each time point, with each replicate consisting of 10 seedlings for both the stems and roots.

Bioinformatics Analysis of *OsMYBdt1*

OsMYBdt1 protein and its homologous sequences were obtained from the Rice Data database. The three-dimensional structure of OsMYBdt1 was generated using the Expasy-SWISS-MODEL. Amino acid sequences of OsMYBdt1 and other MYB transcription factors were aligned using MEGA-X software. Alignment was performed using the neighborhood join method with a bootstrap value of 1000 to evaluate the reliability of the tree topology and deduce evolutionary relationships among the proteins. The phylogenetic tree was visually enhanced using iTOL to improved presentation.

The vectors constructed

BioXM2.6 and high-fidelity Phanta Max Super-Fidelity DNA Polymerase. The vector pRHVnHA was used, and Escherichia coli strain DH5 alpha was employed. The OsMYBdt1 CDS sequence was amplified by PCR using NPB cDNA as a template. Homologous recombination of the linearized vector and the target gene fragment was performed using recombinase at 37℃ for 30 min, followed by transformation into competent E. coli DH5 alpha.

For *OsMYBdt1* knockout vector construction, the Target design website was used to design the knockout target. Competent E. coli DH5 alpha cells were transformed, and positive clones were identified by colony PCR using M13F and target linker primer R. Transgenic plants were generated by infecting calla with Agrobacterium containing the positive clones of the overexpression and knockout vectors, with NPB as the background (Agrobacterium infection was conducted by Beige Biotechnology Co., Ltd., and T0 generation seedlings were provided). All primers used in this study are listed in Table S1.

Subcellular localization of OsMYBdt1

The 276bp coding sequence of OsMYBdt1 was inserted into pRTVcGFP and pRTVnGFP vectors, incorporating green fluorescent protein (GFP) at the C-terminus, resulting in the generation of fusion vectors pRTVcGFP-OsMYBdt1 and pRTVnGFP-OsMYBdt1. Rice protoplasts were separately transformed with the fusion vectors and the empty pRTVcGFP vector as a control. Subsequently, the transformed protoplasts were examined for GFP fluorescence using a laser scanning confocal microscope.

Stomatal observation

A layer of clear nail polish was applied to the lower epidermis of rice leaves for observation. Once dried and formed a film, the mark was removed using transparent adhesive tape to create a temporary mount. Statistical analysis was conducted under a light microscope (400×). For stomatal aperture analysis, the second leaf was taken from 3-week-old seedlings with or without drought treatment, and nail polish impressions were immediately prepared. Stomata were observed using the "instrument", and the proportions of fully open, partially open, and fully closed stomata were calculated. For each line and treatment, at least 50 stomata from 5 independent plants were examined. All experiments were repeated with three independent biological replicates.

Endogenous ABA detection

NPB and transgenic lines were cultured until they reached three weeks of age. The control group remained untreated, while the experimental group was subjected to a 7-day treatment with 20% PEG6000. The determination kit used was the ABA enzyme-linked immunoassay kit (SP29775) from Wuhan Saipei Biotechnology Co., Ltd. (Wuhan, China). For specific guidelines, refer to the official website of Sp Biotech (https://www.spbio.cn).

TB, DAB staining

NPB and transgenic lines after three weeks of culture. The control group remained untreated, while the experimental group was exposed to 20% PEG6000 for 7 days. For TB staining, 5 third leaves were harvested and immersed in 10 ml of 0.1% TB solution. The samples were then subjected to vacuum infiltration for 20-30 minutes to facilitate dye penetration, followed by incubation in darkness for 3d until distinct positive staining was observed.

DAB staining involves treating the leaves with 10 ml of 1 mg/ml DAB solution (pH 3.8, containing 0.05% Tween 20 and 10 mM Na_2HPO_4), followed by vacuum infiltration for 5-10 minutes and incubation in darkness for 3d until brown precipitate appears. After staining, the leaves were rinsed with water, immersed in 10 ml of 95% ethanol in a centrifuge tube, and subjected to decolorization in a water bath at 60-70°C until complete chlorophyll fading. Finally, photographs were captured for observation.

Physiological and Biochemical Index Assays

NPB and transgenic lines, aged 3 weeks, were subjected to different treatments: the control group remained untreated, while the experimental group was exposed to 20% PEG6000 for 7 days. Subsequently, 1 g of leaves from identical positions were placed in 2 ml sterile centrifuge tubes containing pre-sterilized 5mm steel balls. The samples were rapidly frozen in liquid nitrogen and stored at -80℃ for subsequent analysis. After being frozen for 30-60 s, the samples were ground for 60 s at 40 Hz using a grinder, followed by removal and placement on ice for analysis.

The biochemical indicators measured in this experiment were assessed using various biological assay kits, including the malondialdehyde (MDA) content assay kit (AKFA013C), proline (Pro) content assay kit (AKAM003C), superoxide dismutase (SOD) activity assay kit (AKAO001C) and peroxidase (POD) activity assay kit (AKAO005C). All kits were purchased from Beijing Boxbio Science & Technology Co., Ltd. (Beijing, China). The methods for measuring the aforementioned indicators were conducted according to the instructions provided with the reagent kits.

Protein-Protein Docking

The crystal structures of OsRab16A and OsMYBdt1 proteins used in this study were downloaded from the RCSB PDB database. Hdock software was employed for protein-protein docking. Prior to docking, PyMol was used to process the receptor proteins, including removing water molecules, adding hydrogen atoms, and deleting heteroatoms. After docking, Prodigy was used to calculate the binding energy, and PyMol was finally employed for visual analysis of the docking results.

Dual-LUC Assay

The Rab16a promoter was inserted into the pGreenII 0800-LUC vector to construct the reporter plasmid. The coding sequences of OsMYBdt1 was cloned and inserted into the pGreenII 62-SK vector. These recombinant plasmids were subsequently transferred into A. tumefaciens (EHA105). Tobacco leaves were co-infiltrated with the Agro-bacterium suspension. Luminescence activity was evaluated using a bioluminescence imaging system 48 h post-infiltration.Simultaneously, infiltrated tobacco leaf samples

were collected and assayed for luciferase activity using the Dual-Luciferase Reporter Assay Kit (Promega, America).

Statistical Analyses

Each experiment in the study comprised three biological replicates. Statistical analysis was performed using IBM SPSS Statistics 25 software, involving a one-way ANOVA followed by either a t-test or Duncan's multiple comparison test.

Declarations

CRediT authorship contribution statement

Guangzhou Li: Writing - Original draft, Writing - Review &Editing, Visualization, Methodology, Investigation, Data Curation. Shipeng Huang: Validation, Investigation, Data curation. Su Jiang: Methodology, Validation, Investigation, Data curation. Chuanxin Chen: Writing - Review & Editing, Validation, Data Curation. Yancheng Sun: Methodology, Investigation, Data Curation. Tuo Zhong: Visualization, Methodology, Data curation. Xin Tian: Data Curation. Guanghui Chen and Dan Wang: Writing - Review & Editing, Supervision, Resources, Conceptualization. Chenggang Li: Writing - Review & Editing, Validation, Supervision. Fenglin Huang：Funding acquisition, Resources. Huqiang He：Data curation, Conceptualization. Yue Wang：Validation, Data curation. Yajun Hu：Investigation, Data Curation.

Conflict of interest

The authors declare that the research was conducted in the absence of any commercial or financial relationships that could be construed as potential conflicts of interest.

Acknowledgments

We thank Dr. Yuese Ning (Institute of Plant Protection, Chinese Academy of Agricultural Sciences) for generously providing a series of vectors, including the complementary vectors, the CRISPR/Cas9 genome editing vectors and ectopic expression vectors. This work was supported by grants from the Natural Science Foundation of Hunan Agriculture University (25KJ016) and Agricultural Science and Technology Innovation Fund Project of Hunan Province （2025CX79 and 2024CX17）.

References

1. Baldoni, E., Genga, A., Cominelli, E. 2015. Plant MYB Transcription Factors: Their Role in Drought Response Mechanisms. Int. J. Mol. Sci. 16(7). https://doi.org/10.3390/ijms160715811.
2. Chen, G., He, W., Guo, X., Pan, J. 2021. Genome-Wide Identification, Classification and Expression Analysis of the MYB Transcription Factor Family in Petunia. Int. J. Mol. Sci. 22(9), 4838. https://doi.org/10.3390/ijms22094838.

3. Cutler, S. R., Rodriguez, P. L., Finkelstein, R. R., Abrams, S. R. 2010. Abscisic acid: emergence of a core signaling network. Annu. Rev. Plant Biol. 61, 651–679. https://doi.org/10.1146/annurev-arplant-042809-112122.
4. Fu, X., Liu, C., Li, Y., Liao, S., Cheng, H., Tu, Y., Zhu, X., Chen, K., He, Y., Wang, G., 2021. The coordination of *OsbZIP72* and *OsMYBS2* with reverse roles regulates the transcription of OsPsbS1 in rice. New Phytol. 229(1), 370–387. https://doi.org/10.1111/nph.16877.
5. Fujii, H., Chinnusamy, V., Rodrigues, A., Rubio, S., Antoni, R., Park, S. Y., Cutler, S. R., Sheen, J., et al., 2009. In vitro reconstitution of an abscisic acid signalling pathway. Nature. 462(7273), 660–664. https://doi.org/10.1038/nature08599.
6. Fujita, Y., Fujita, M., Satoh, R., Maruyama, K., Parvez, M. M., Seki, M., Hiratsu, K., Ohme-Takagi, M., Shinozaki, K., et al., 2005. *AREB1* is a transcription activator of novel ABRE-dependent ABA signaling that enhances drought stress tolerance in Arabidopsis. Plant Cell. 17(12), 3470–3488. https://doi.org/10.1105/tpc.105.035659.
7. Fujita, Y., Fujita, M., Satoh, R., Maruyama, K., Parvez, M. M., Seki, M., Hiratsu, K., Ohme-Takagi, M., Shinozaki, K., Yamaguchi-Shinozaki, K. (2005). AREB1 is a transcription activator of novel ABRE-dependent ABA signaling that enhances drought stress tolerance in Arabidopsis. The Plant cell, 17(12), 3470–3488. https://doi.org/10.1105/tpc.105.035659
8. Gao, L., Lv, Q., Wang, L., Han, S., Wang, J., Chen, Y., Zhu, W., Zhang, X., Bao, F., Hu, Y., et al., 2024. Abscisic acid-mediated autoregulation of the MYB41-BRAHMA module enhances drought tolerance in Arabidopsis. Plant Physiol. 196(2), 1608–1626. https://doi.org/10.1093/plphys/kiae383.
9. Geng, A.; Lian, W.; Wang, Y.; Liu, M.; Zhang, Y.; Wang, X.; Chen, G. 2024. Molecular Mechanisms and Regulatory Pathways Underlying Drought Stress Response in Rice. Int. J. Mol. Sci. 25, 1185. https://doi.org/10.3390/ijms25021185.
10. Kang L, Teng Y, Cen Q, 2022.Genome-Wide Identification of R2R3-MYB Transcription Factor and Expression Analysis under Abiotic Stress in Rice. Plants (Basel). 11(15):1928. https://doi.org/10.3390/plants11151928.
11. Katiyar, A., Smita, S., Lenka, S. K., Rajwanshi, R., Chinnusamy, V., Bansal, K. C., 2012. Genome-wide classification and expression analysis of MYB transcription factor families in rice and Arabidopsis. BMC Genomics, 13, 544. https://doi.org/10.1186/1471-2164-13-544.
12. Li ZK, Gao YM., 2009. Molecular breeding for drought-tolerant rice (*Oryza sativa* L.): progress and perspectives. In: Drought Frontiers in Rice. Singapore: World Scientific. 91-112. https://doi.org/10.1142/9789814280013_0006.
13. Li, R., Song, Y., Wang, X., Zheng, C., Liu, B., Zhang, H., Ke, J., Wu, X., Wu, L., Yang, R., et al., 2024. *OsNAC5* orchestrates *OsABI5* to fine-tune cold tolerance in rice. J. Integr. Plant Biol. 66(4), 660–682. https://doi.org/10.1111/jipb.13585.
14. Liu, J., Osbourn, A., Ma, P. 2015. MYB Transcription Factors as Regulators of Phenylpropanoid Metabolism in Plants. Mol. Plant 8(5), 689–708. https://doi.org/10.1016/j.molp.2015.03.012.

15. Lv, Y., Yang, M., Hu, D., Yang, Z., Ma, S., Li, X., Xiong, L. 2017. The *OsMYB30* Transcription Factor Suppresses Cold Tolerance by Interacting with a JAZ Protein and Suppressing β-Amylase Expression. Plant Physiol. 173(2), 1475–1491. https://doi.org/10.1104/pp.16.01725.
16. Miller, G., Suzuki, N., Ciftci-Yilmaz, S., Mittler, R., 2010. Reactive oxygen species homeostasis and signalling during drought and salinity stresses. Plant Cell Environ. 33(4), 453–467. https://doi.org/10.1111/j.1365-3040.2009.02041.x.
17. Mundy J, Chua NH. 1988. Abscisic acid and water-stress induce the expression of a novel rice gene. The EMBO Journal. 7, 2279–2286. https://doi.org/10.1002/j.1460-2075.1988.tb03070.x.
18. Nakabayashi, R., Yonekura-Sakakibara, K., Urano, K., Suzuki, M., Yamada, Y., Nishizawa, T., Matsuda, F., Kojima, M., Sakakibara, H., Shinozaki, K., et al., 2014. Enhancement of oxidative and drought tolerance in Arabidopsis by overaccumulation of antioxidant flavonoids. Plant J. 77(3), 367–379. https://doi.org/10.1111/tpj.12388.
19. Nam, K. H., Li, J., 2002. BRI1/BAK1, a receptor kinase pair mediating brassinosteroid signaling. Cell. 110(2), 203–212. https://doi.org/10.1016/s0092-8674(02)00814-0.
20. Ono, A., Izawa, T., Chua, N. H., Shimamoto, K., 1996. The *rab16B* promoter of rice contains two distinct abscisic acid-responsive elements. Plant Physiol. 112(2), 483–491. https://doi.org/10.1104/pp.112.2.483.
21. Peng, W., Zhang, Y., Xie, H., Yu, Y., Zhu, M., 2025. Research progress on the synergistic regulation of MYB transcription factor-mediated developmental plasticity and stress responses in rice. Front. Plant Sci. 16, 1668800. https://doi.org/10.3389/fpls.2025.1668800.
22. Post-Beittenmiller D. 1996. BIOCHEMISTRY AND MOLECULAR BIOLOGY OF WAX PRODUCTION IN PLANTS. Annu Rev Plant Physiol Plant Mol Biol. 47, 405–430. https://doi.org/10.1146/annurev.arplant.47.1.405.
23. Sandhu, N., Dixit, S., Swamy, B. P. M., Raman, A., Kumar, S., Singh, S. P., Yadaw, R. B., Singh, O. N., Reddy, J. N., Anandan, A., et al., 2019. Marker Assisted Breeding to Develop Multiple Stress Tolerant Varieties for Flood and Drought Prone Areas. Rice (N.Y.) 12(1), 8. https://doi.org/10.1186/s12284-019-0269-y.
24. Seo, P.J., Lee, S.B., Suh, M.C., Park, M., Go, Y.S., Park, C., 2011. The *MYB96* Transcription Factor Regulates Cuticular Wax Biosynthesis under Drought Conditions in *Arabidopsis.* Plant Cell. 23, 1138 - 1152. https://doi.org/10.1105/tpc.111.083485.
25. Shinozaki, K., Yamaguchi-Shinozaki, K., 2007. Gene networks involved in drought stress response and tolerance. J. Exp. Bot. 58(2), 221–227. https://doi.org/10.1093/jxb/erl164.
26. Umezawa, T., Sugiyama, N., Mizoguchi, M., Hayashi, S., Myouga, F., Yamaguchi-Shinozaki, K., Ishihama, Y., Hirayama, T., Shinozaki, K., 2009. Type 2C protein phosphatases directly regulate abscisic acid-activated protein kinases in Arabidopsis. Proc. Natl. Acad. Sci. U.S.A. 106(41), 17588–17593. https://doi.org/10.1073/pnas.0907095106.
27. Upadhyaya, G., Das, A., Ray, S., 2021. A rice R2R3-MYB (*OsC1*) transcriptional regulator improves oxidative stress tolerance by modulating anthocyanin biosynthesis. Physiol. Plant. 173(4), 2334–

2349. https://doi.org/10.1111/ppl.13583.

28. Wang, D., Liu, Z., Xiao, Y., Liu, X., Chen, Y., Zhang, Z., Kang, H., Wang, X., Jiang, S., Peng, S., Tan, X., Zhang, D., Liu, Y., Wang, G. L., & Li, C. (2021). Association Mapping and Functional Analysis of Rice Cold Tolerance QTLs at the Bud Burst Stage. Rice (New York, N.Y.), 14(1), 98. https://doi.org/10.1186/s12284-021-00538-0.
29. Wang, Q., Guan, Y., Wu, Y., Chen, H., Chen, F., Chu, C., 2008. Overexpression of a rice *OsDREB1F* gene increases salt, drought, and low temperature tolerance in both Arabidopsis and rice. Plant Mol. Biol. 67(6), 589–602. https://doi.org/10.1007/s11103-008-9340-6.
30. Watanabe KA, Homayouni A, Gu L, Huang KY, Ho TD, Shen QJ, 2017. Transcriptomic analysis of rice aleurone cells identified a novel abscisic acid response element. Plant Cell Environ. 40(9):2004-2016. https://doi.org/10.1111/pce.13006.
31. Wu, S., Hu, C., Tan, Q., Xu, S., Sun, X., 2017. Nitric Oxide Mediates Molybdenum-Induced Antioxidant Defense in Wheat under Drought Stress. Front. Plant Sci. 8, 1085. https://doi.org/10.3389/fpls.2017.01085.
32. Xiong, H., Li, J., Liu, P., Duan, J., Zhao, Y., Guo, X., Li, Y., Zhang, H., Ali, J., Li, Z., 2014. Overexpression of *OsMYB48-1*, a novel MYB-related transcription factor, enhances drought and salinity tolerance in rice. PLoS ONE. 9(3), e92913. https://doi.org/10.1371/journal.pone.0092913.
33. Yamaguchi-Shinozaki, K., Shinozaki, K. 2005. Organization of cis-acting regulatory elements in osmotic- and cold-stress-responsive promoters. Trends Plant Sci. 10, 88-94. https://doi.org/10.1016/j.tplants.2004.12.012.
34. Yang, A., Dai, X., Zhang, W. H. 2012. A R2R3-type MYB gene, *OsMYB2*, is involved in salt, cold, and dehydration tolerance in rice. J. Exp. Bot. 63(7), 2541–2556. https://doi.org/10.1093/jxb/err431
35. Yin, X., Cui, Y., Wang, M., Xia, X., 2017. Overexpression of a novel MYB-related transcription factor, *OsMYBR1*, confers improved drought tolerance and decreased ABA sensitivity in rice. Biochem. Biophys. Res. Commun. 490(4), 1355–1361. https://doi.org/10.1016/j.bbrc.2017.07.029.
36. Yoshida, T., Mogami, J., Yamaguchi-Shinozaki, K., 2014. ABA-dependent and ABA-independent signaling in response to osmotic stress in plants. Curr. Opin. Plant Biol. 21, 133–139. https://doi.org/10.1016/j.pbi.2014.07.009.
37. Zhao, H., Yao, P., Zhao, J., Wu, H., Wang, S., Chen, Y., Hu, M., Wang, T., Li, C., Wu, Q., 2022. A Novel R2R3-MYB Transcription Factor *FtMYB22* Negatively Regulates Salt and Drought Stress through ABA-Dependent. Pathway. Int. J. Mol. Sci. 23(23), 14549. https://doi.org/10.3390/ijms232314549.

Figures

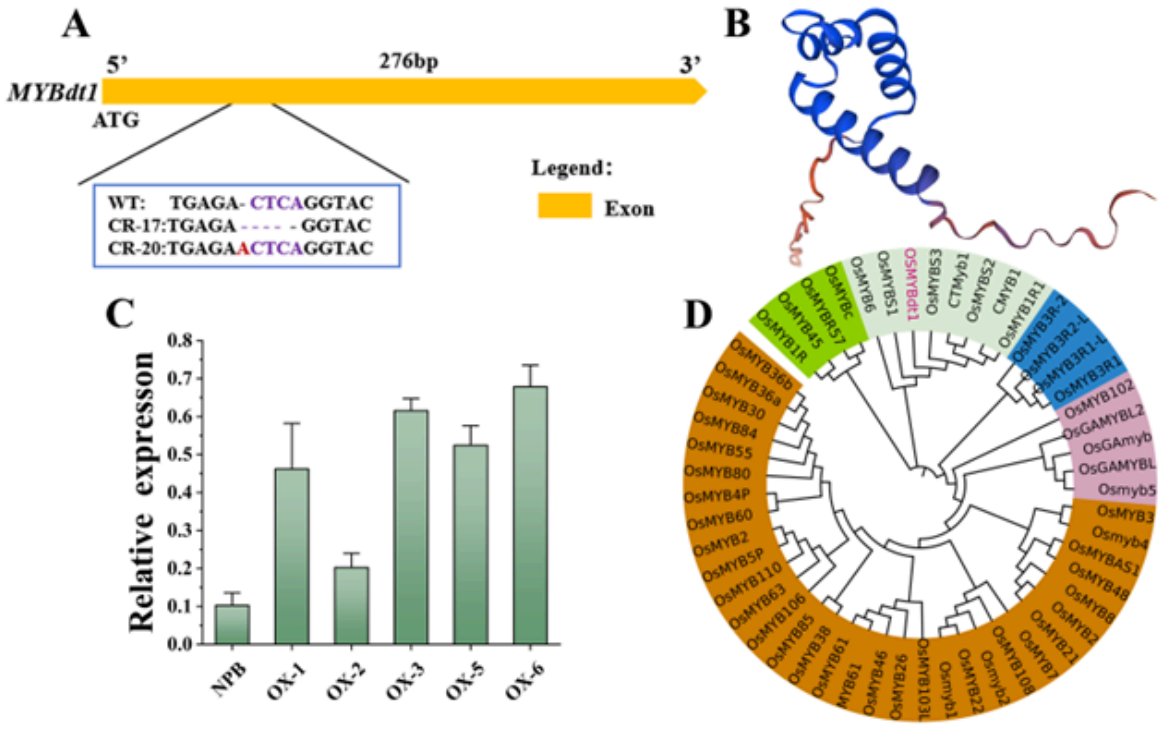


Fig. 1. Bioinformatic and phylogenetic analyses of *OsMYBdt1*. A: Structural representation of *OsMYBdt1*, encoding 276 amino acids in a single exon. Highlighted are deletion and insertion amino acid sequences in two knockout homozygous lines (CR-17, CR-20). B: Expression patterns of *OsMYBdt1* overexpressing lines. C: Three-dimensional structural depiction of *OsMYBdt1*. The blue spiral region represents the DNA domain of MYB, while the reddish-brown flexible region indicates the non-conserved regulatory region. D: Phylogenetic tree illustrating the relationship between *OsMYBdt1* and other members of the MYB family.

Figure 1

See image above for figure legend

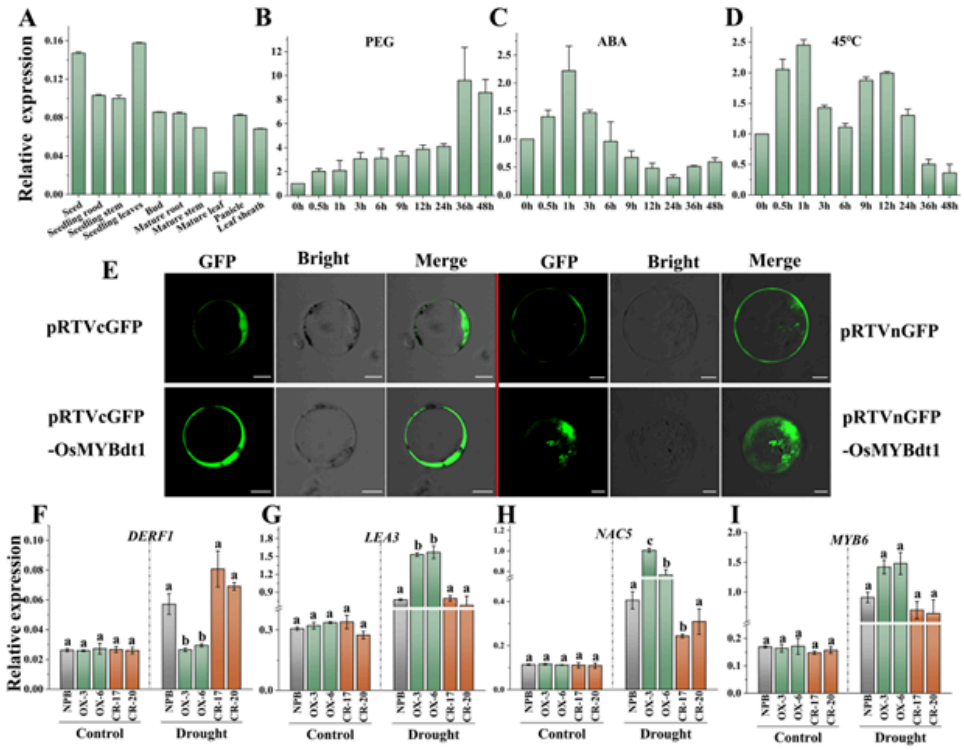


Fig. 2. Expression analysis and subcellular localization of the *OsMYBdt1* gene. A: Expression levels of *OsMYBdt1* across various time points and tissues. B: Expression level of *OsMYBdt1* from 0h to 48h following treatment with 20% PEG6000. C: Expression level of *OsMYBdt1* from 0h to 48h following treatment with 200 μmol/L ABA. D: Expression level of *OsMYBdt1* under 45°C treatment. E: Subcellular localization of *OsMYBdt1*. Using the empty pRTVcGFP and pRTVnGFP vectors as controls, the fusion vector (pRTVcGFP-OsMYBdt1) and the empty vector were individually transformed into rice protoplasts. Merge indicates the merged GFP and bright field images. Was mainly localized to the plasma membrane and displayed a ring-shaped signal. In contrast, OsMYBdt1-GFP fluorescence was observed in both the cytoplasm and nucleus. F-I: Relative expression levels of *DERF1* (F), *LEA3* (G), *NAC5* (H), *MYB6* (I) in control and drought-treated samples. Each column represents an average of three replicates, and bars indicate the SD. Different letters (a, b, c) indicate significant differences.

Figure 2

See image above for figure legend

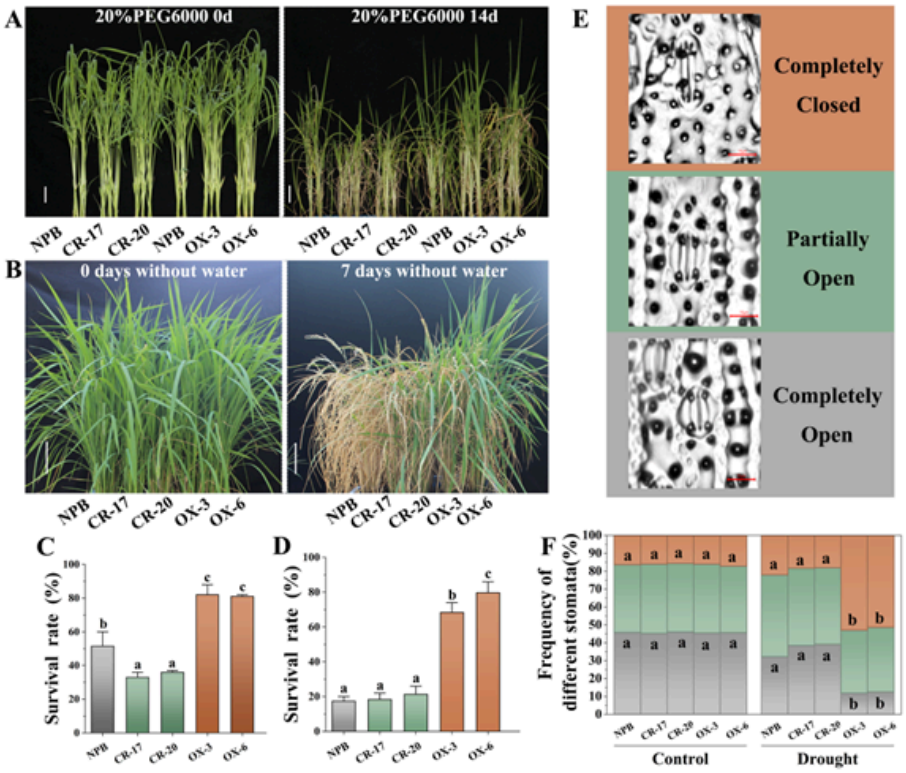


Fig. 3. llustrates the enhanced drought stress tolerance in rice plants conferred by *OsMYBdt1*. A: Depicts the phenotypic changes in 3-week-old seedlings exposed to 20% PEG 6000 for days compared to those treated for 14 days and then allowed to recover for 7 days. Scale bar = 2 cm. B: Shows the plant phenotypes before and after a 7 day water withholding period during the heading stage. Scale bar = 10 cm. C: Presents the recovery of 3-week-old seedlings treated with 20% PEG6000 for 14 days in terms of a 7-day survival rate. D: Exhibits the survival rates of plants at the heading stage following 7 days of rewatering. E: Field emission scanning electron microscopy images of three states of stomatal activity (completely open, partially open, and completely closed). Scale corresponds to 10 µM. F: Percentage of stomata at three possible states (completely open, partially open, and completely closed) under control conditions and drought treatment (20% PEG6000) in NPB, *osmybdt1*CR and *OsMYBdt1*OX line.

Figure 3

See image above for figure legend

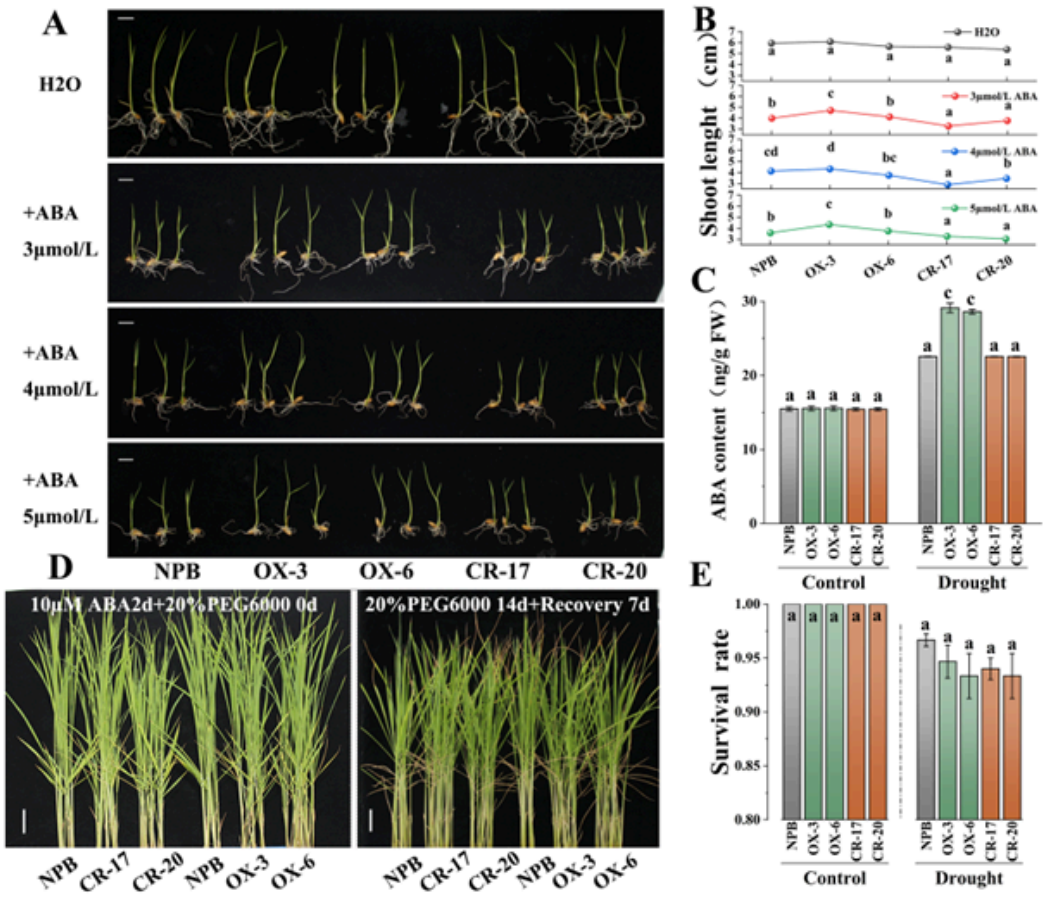


Fig. 4. Exogenous ABA enhanced the drought stress resistance of OsMYBdt1CR. A: Bud stage phenotypes of the control and treatment groups under varying ABA concentrations. Scale bar = 1 cm. B: Bud lengths of plants at the bud stage in both the control and treatment groups across different ABA concentrations. C: Endogenous ABA content in three-week-old seedlings from the control and treatment groups before treatment and following recovery. D: Phenotypes of plants at the seedling stage after the external application of ABA. Scale bar = 2 cm. E: Survival rates of plants at the seedling stage after the external application of ABA.

Figure 4

See image above for figure legend

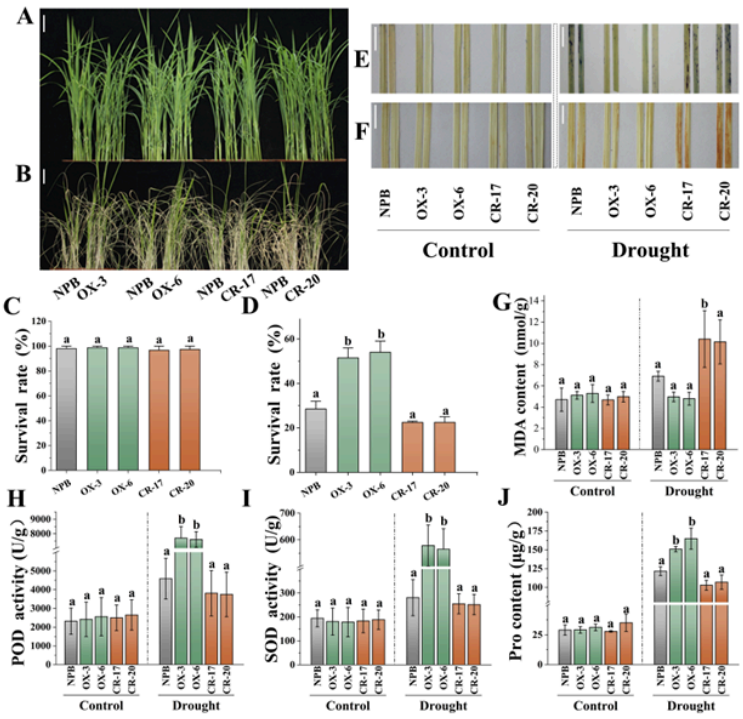


Fig. 5. *OsMYBdt1* mitigates drought sensitivity through the modulation of antioxidant enzymes. A: Phenotypes of three-week-old, soil-cultured NPB, two *OsMYBdt1*OX, and two *osmybdt1*CR seedlings. Scale bar = 2 cm. B: Phenotypes of soil-grown seedlings following 12 days of water deprivation and 7 days of rewatering. Scale bar = 2 cm. C: Three-week survival rates of soil-cultured NPB, two *OsMYBdt1*OX, and two *osmybdt1*CR seedlings. D: Survival rates of soil-grown seedlings after 12 days of water deprivation and 7 days of rewatering. E-F: Twenty percent 20% PEG6000 was utilized to stain the rice leaves of both the treatment and control groups under simulated drought stress, employing trypan blue (TB) (E) and 3,3'-diaminobenzidine (DAB) (F). Scale bar = 1 cm. G-J: Variations in the activities of malondialdehyde (MDA) (G), peroxidase (POD) (H), superoxide dismutase (SOD) (I), and proline (Pro) (J) in both the control and treatment groups under normal and drought stress conditions.

Figure 5

See image above for figure legend

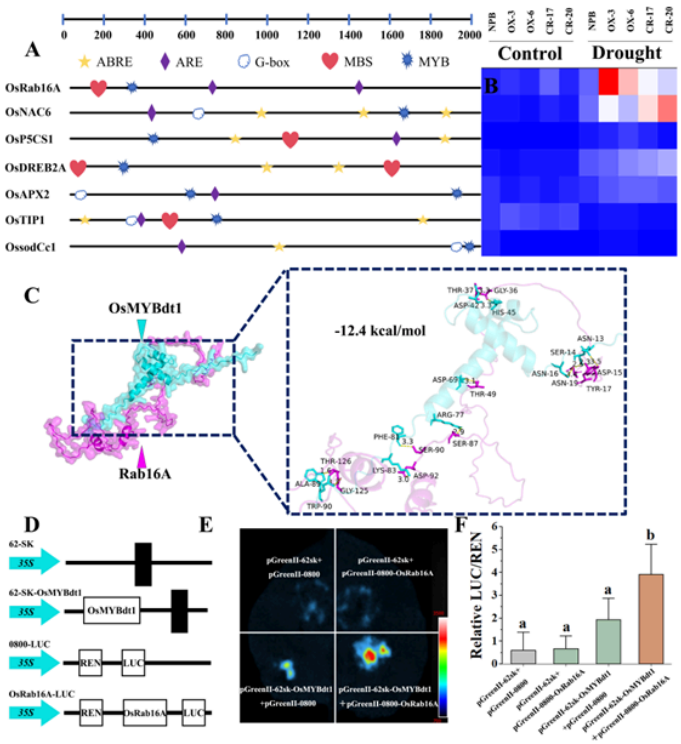


Fig. 6. Exploration of *OsMYBdt1* interacting genes. A: The promoter sequence upstream of the transcription start site (2 kb) was obtained using Phytozome, and cis-acting element analysis was performed with PlantCARE. B: Expression levels of *OsMYBdt1* in control and treated groups under normal stress and drought stress conditions were analyzed for *OsNAC6*, *OsRab16A*, *OsDREB2A*, *OsP5CS1*, *OsAPX2*, *OssodCc1*, and *OsTIP1*. C: Binding mode of *OsRab16A* and *OsMYBdt1* obtained from docking. The left panel shows the overall view, and the right panel shows the local view. The cyan and pink cartoons represent *OsMYBdt1*、*OsRab16* protein, respectively. The yellow indicate the distances between atoms (unit: Å), which are used to show the strength and position of interactions such as hydrogen bonds and hydrophobic interactions.In this complex, Prodigy calculated that the binding energy between OsRab16A and OsMYBdt1 is -12.4 kcal/mol. D: Schematic diagram of the dual luciferase reporter assay. Effector: pGreenII-62-SK-OsMYBdt1; Reporter: pGreenII-0800-LUC (proOsRab16A::LUC, 35S::REN). Four combinations were co-transformed into rice protoplasts as indicated. E: LUC fluorescence imaging of rice protoplasts co-transformed with the indicated effector and reporter constructs. The four quadrants correspond to the four combinations described in (D). Fluorescence intensity reflects the transcriptional activity of proOsRab16A. F: Relative LUC/REN activity of the dual luciferase reporter assay. The LUC/REN ratio was calculated to normalize transfection efficiency. Data are mean ± SD (n = 3). Different letters indicate significant differences at $P < 0.05$ (one-way ANOVA).

Figure 6

See image above for figure legend

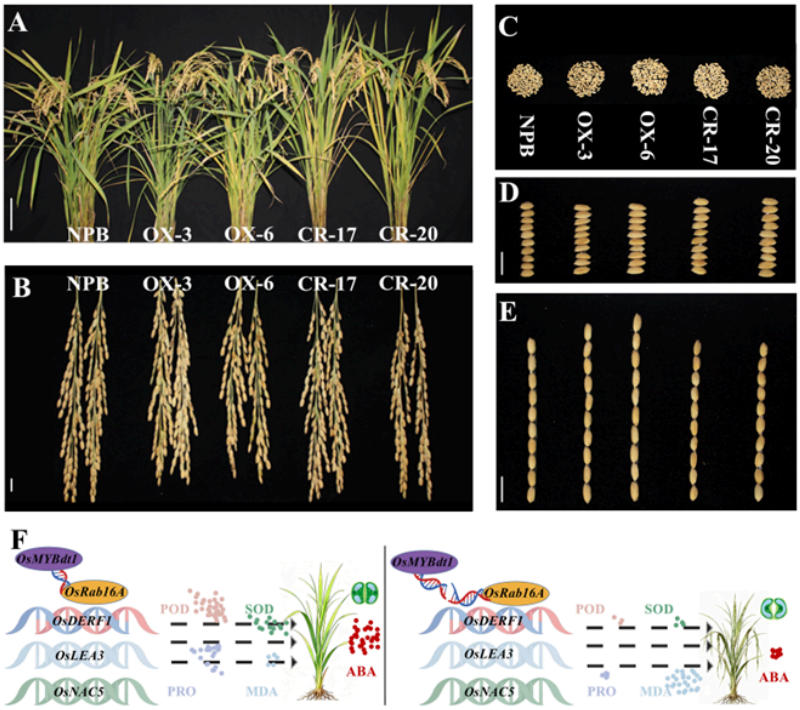


Fig. 7. *OsMYBdt1* mediates drought resistance and agronomic traits in rice. A: Plant height phenotypes of NPB, two *OsMYBdt1*OX lines, and two *osmybdt1*CR lines. Scale bar = 2 cm. B:Panicle length of NPB, two *OsMYBdt1*OX lines, and two *osmybdt1*CR lines. Scale bar = 1 cm. C: Range of 100-seed. D-E: Grain length and grain width phenotypes of NPB, two *OsMYBdt1*OX lines, and two *osmybdt1*CR lines. Scale bar = 1 cm. F: The diagram presents a comparative view of the *OsMYBdt1*OX and *osmybdt1*CR under drought stress conditions.In *OsMYBdt1*OX plants, *OsMYBdt1* activates *OsRab16A*, an ABA-responsive gene, leading to elevated endogenous ABA levels. This ABA-mediated signaling pathway is further amplified through the transcriptional activation of *OsNAC5*. Concurrently, *OsMYBdt1* modulates the expression of other stress-responsive genes, including downregulation of *OsDERF1* and upregulation of *OsLEA3*. These transcriptional changes collectively enhance antioxidant defense systems, as evidenced by increased activities of POD, SOD, and Pro accumulation, while reducing MDA formation and associated membrane damage. *OsMYBdt1*OX plants predominantly display closed stomata under drought conditions, effectively reducing transpirational water loss and maintaining turgid, healthy leaves. In contrast, *osmybdt1*CR mutants exhibit predominantly open or partially closed stomata, leading to excessive water loss and wilted, chlorotic phenotypes.

Figure 7

See image above for figure legend

Supplementary Files

This is a list of supplementary files associated with this preprint. Click to download.

- OsMYBdt1primersequences.xlsx
- S1.6.15.pptx
- S26.15.pptx
- S36.15.pptx